SILK RESERVOIRS FOR LOCAL DELIVERY OF CISPLATIN FOR NEUROBLASTOMA TREATMENT: IN VITRO AND IN VIVO EVALUATIONS

Burcin Yavuz, PhD[1], **Jasmine Zeki, BS**[2], **Jordan Taylor, MD**[2], **Kristin Harrington**[1], **Jeannine M. Coburn, PhD**[1,3], **Naohiko Ikegaki, PhD**[4], **David L. Kaplan, PhD**[1,*], and **Bill Chiu, MD**[2,*]

[1]Department of Biomedical Engineering, Tufts University, Medford, MA, USA

[2]Department of Surgery, Stanford University, Stanford, CA, USA

[3]Department of Biomedical Engineering, Worcester Polytechnic Institute, Worcester, MA, USA

[4]Department of Anatomy and Cell Biology, University of Illinois at Chicago, Chicago, IL, USA

Abstract

Neuroblastoma is the most common extra-cranial childhood tumor and current treatment requires surgical resection and multi-drug chemotherapy. Local, perioperative delivery of chemotherapeutics is a promising treatment method for solid tumors that require surgical removal. In this study we have aimed to develop a controlled release implant system to deliver cisplatin in tumor/tumor resection area. Silk fibroin, a biodegradable, non-immunogenic biopolymer was employed to encapsulate different doses of cisplatin in a reservoir system. The physical integrity of the reservoirs was characterized by evaluating the crystalline structure of silk secondary structure using Fourier Transform Infrared (FTIR) spectroscopy. The in vitro release of cisplatin was evaluated in phosphate buffered saline at 37°C and the reservoirs were able to release the drug up to 30 days. The cytotoxicity of cisplatin and cisplatin reservoirs were tested on KELLY cells. Cytotoxicity data showed 3.2 μg/mL cisplatin was required to kill 50 percent of the cell population and the released cisplatin from the silk reservoirs showed significant cytotoxicity up to 21 days. Intratumoral implantation of silk reservoirs into an orthotopic neuroblastoma mouse model decreased tumor growth significantly when compared to controls. These results suggest that silk reservoirs are promising carriers for cisplatin delivery to the tumor site.

Keywords

Cancer chemotherapy; drug delivery system; biomaterials; controlled release; solid dosage forms; site-specific delivery

---

*Co-Corresponding Authors: David L. Kaplan, PhD, Department of Biomedical Engineering, Tufts University, 4 Colby Street, Medford, MA 02155, Phone: 617-627-3251, david.kaplan@tufts.edu, Bill Chiu, MD, Department of Surgery, Stanford University, 300 Pasteur Drive, Alway M116, Phone: 650-723-6439, bhsc@stanford.edu.

INTRODUCTION

Neuroblastoma is the most common pediatric extracranial solid tumor that can be located in a variety of places in the body, including the thoracic cavity, adrenal medulla and sympathetic chain[1]. Fifteen percent of pediatric cancer-related deaths occur due to neuroblastoma and the overall survival rate is 36% in high-risk groups[2]. Patients with the high-risk disease are treated with an aggressive, multimodal therapy (including chemotherapy, radiation therapy and immunotherapy) following surgical removal of the tumor. Systemic chemotherapy involves multiagents (such as cyclophosphamide, topotecan, cisplatin, doxorubicin, vincristine and etoposide) and predisposes patients to long- and short-term toxicities such as renal toxicity, cardiotoxicity, infection, and gastrointestinal symptoms[3–5]. The development of carrier platforms that can deliver drugs to the tumor site, maximize tumor cell death and minimize systemic side effects are essential for higher survival rates as well as improved quality of life of the patients[6–10].

Cisplatin (cis diamminedichloro platinum (II)) is one of the most commonly used chemotherapy drugs for the treatment of various solid tumors including neuroblastoma. However, a short serum half-life and high protein binding (up to 90%) causes major problems in cisplatin efficacy[11]. Furthermore cisplatin use is limited due to acquired resistance and severe adverse effects including, but not limited to, nausea, vomiting, neurotoxicity, nephrotoxicity and ototoxicity[12]. Various approaches including microparticles, nanoparticles, liposomes, micelles and dendrimer conjugates have been investigated in order to improve systemic efficacy of cisplatin[13–17]. However, severe toxic side effects are persistent for both cisplatin and cisplatin analogues (carboplatin, nadaplatin)[18] and there is still a need for an alternative delivery system for cisplatin. While the search continues for a systemic formulation, intra-tumoral applications are being investigated as an alternative to deliver cisplatin into the target site[19, 20]. Intra-tumoral treatment may also help decrease acquired resistance by allowing for higher intra-tumoral concentrations, better eradicating tumor cells that might survive at lower concentrations[9].

Silk fibroin (silk) is an Food and Drug Administration (FDA) approved biomaterial for some medical devices and this biomaterial has been employed for various applications like drug delivery, tissue regeneration and bioactive coatings due to favorable properties such as biocompatibility, biodegradability, controllable drug loading and release, low immune response, low cost and formulation versatility[21–24]. Silk already has been successfully used for controlled delivery of chemotherapeutic drugs, especially hydrophobic molecules that have a high affinity to silk[25–30]. We have previously formulated doxorubicin, vincristine and etoposide with silk platforms and achieved decreased tumor growth and/or longer animal survival after intra-tumoral implantation into an orthotopic neuroblastoma model[7–10, 28, 31]. Notably, we have been able to significantly decrease orthotopic tumor growth with local therapy relative to control while reducing the systemic exposure to these toxic chemotherapies[9].

In this study, we hypothesized that entrapping high dose cisplatin in powder format within a silk reservoir would help with solubility of cisplatin and provide controlled release. Furthermore we hypothesized that implanting this system directly into the center of an

orthotopic human neuroblastoma tumor in mice would facilitate improved outcomes by achieving high drug concentrations within the tumor to decrease tumor growth rate.

MATERIALS AND METHODS

Silk Fibroin Isolation

Silk fibroin was isolated from *Bombyx mori* cocoons as previously described[21]. Cocoons were cut into pieces and degummed for 30 minutes by boiling in 0.02 M Na_2CO_3 (Sigma, St. Louis, MO, USA) and then washed with distilled water to rinse and remove sericin proteins. Silk fibers were dried overnight with air-drying, then 1 g of the dried silk fibroin was dissolved in 4 mL of 9.3 M lithium bromide (Sigma, St. Louis, MO, USA) for 4 hours at 60°C. This solution was dialyzed (Pierce 3.4 kDa MWCO dialysis cassette; Fisher Scientific, Pittsburg, PA) against distilled water for 2 days to remove the salt where the water was replaced 6 times during the 2 days period. One mL of the prepared silk fibroin (silk) solution was weighed before and after drying to calculate the final silk concentration of the solution, diluted to 6% with ultra purified water and stored at 4°C until use.

Preparation of silk reservoirs

For fabrication of cisplatin (Sigma, St. Louis, MO, USA) loaded silk reservoirs, 100μL of 6% (w/v) sterile (filtered) silk solution was pipetted in 96 well plates, kept at −80°C until frozen and then lyophilized to form blank silk foams. Reservoirs consisted of three layers of silk foams with cisplatin being entrapped in the middle layer. A pocket has been created in the second foam layer using a 1.5 mm diameter punch and cisplatin was accurately weighed (0.2, 0.5, 1 and 2 mg) and placed into the punctured layer. These three layers of foam (blank-cisplatin-blank) were then manually compressed together for 30 seconds to entrap cisplatin inside the two blank layers of foam to form a mini tablet shaped cisplatin reservoir with 6×2 mm diameters (Figure 1). Reservoirs were then water vapor annealed overnight in a vacuum oven at room temperature to induce the crystallinity of silk.

Fourier Transform Infrared (FTIR) Spectroscopy

The physical structure of the silk reservoirs with or without cisplatin were evaluated using FTIR Spectroscopy (JASCO FTIR 6200 spectrometer, Jasco, USA) and β-sheet crystalline fractions was determined as described previously[32]. Before all sample measurements, background was collected. The amide I region (1605 – 1705 cm^{-1}) of silk fibroin was deconvoluted using OPUS 5.0 software (Bruker Optics, USA) fourier self deconvolution method with Lorentzian line. Side chains (1605–1615 cm^{-1}), beta sheets (1622–1637 cm^{-1}), random coils (1638–1655 cm^{-1}), alfa helixes (1656–1662 cm^{-1}) and turns (1663–1696 cm^{-1}) were described for each formulation. IBM SPSS Statistics 22 Software (New York, USA) was used to perform One Way ANOVA for statistical analysis ($p < 0.05$) of the FTIR results.

In Vitro Release Studies

For in vitro release studies, reservoirs were placed in Eppendorf tubes (1.5mL) individually and incubated in 100μL phosphate buffered saline (PBS), pH 7.4 (Life Technologies, Grand Island, NY) at 37°C. PBS was collected at every time point and replaced with fresh medium.

The time points for sample collections were 2, 5, 24 hours, 1 day, 2, 3, 6, 8, 10, 13, 15, 20, 24, 27 and 30 days. Following collection release samples were stored at −80°C until quantification. Cisplatin was quantified using a colorimetric method based on ligand exchange reaction of cisplatin with o-phenylenediamine (o-PDA, Sigma, St. Louis, MO, USA)[33]. Briefly, 100μL cisplatin solution was mixed with 1 mL 1.4 mg/mL o-PDA and 2 mL pH 6.8 phosphate buffer and heated for 30 min at 90°C until the samples gave a yellow/green color. Then the absorbance was read at 706 nm using ultraviolet/visible light spectroscopy (SpectraMax M2e, Molecular Devices, Sunnyvale, CA, USA). The in vitro release studies were performed with 3 replicates and blank reservoir release samples were used for background correction. IBM SPSS Statistics 22 Software (New York, USA) was used to perform One Way ANOVA and for statistical analysis and Tukey-b posthoc analysis was used to evaluate the differences between groups ($p < 0.05$).

In Vitro Cytotoxicity Studies

Cytotoxicity of cisplatin and cisplatin loaded silk reservoirs on human neuroblastoma KELLY cells (Sigma-Aldrich, St Louis, MO) were evaluated using AlamarBlue® assay (Invitrogen, Carlsbad, CA). RPMI 1640 with GlutaMAX (Gibco, Grand Island, NY) supplemented with 10% fetal bovine serum, 100 IU/ml penicillin and 100 μg/ml streptomycin was used to maintain the cells that were incubated at 37°C, in a 5% CO_2 atmosphere. Once the cells reach 80% confluence, they were passaged using Trypsin-EDTA 0.25% (Gibco, GrandIsland, NY). For evaluation of cisplatin cytotoxicity, the cells were exposed to varying concentrations of cisplatin in a range of 1ng/mL to 50μg/mL in culture medium described above (n=4) and LC50 (lethal concentration to kill 50% of the cells) was calculated. Toxicity of cisplatin reservoirs were tested by exposing the cells to in vitro release samples of each formulation in triplicate. For AlamarBlue® assay, 10,000 KELLY cells (P7) per well were seeded in 96-well plates and incubated overnight to attach and adhere the plates. Culture medium was removed and either cisplatin solutions in medium (100 μL, 1ng/mL to 50μg/mL) or medium plus the cisplatin release samples (1:1, 100 μL medium + 100 μL release sample) were added to the cells. The plates were incubated 48 hours in presence of cisplatin samples before adding 10% AlamarBlue® solution and incubating an additional 4 hours at 37°C as suggested by the manufacturer's protocols. A plate reader (SpectraMax m2e, Molecular Devices) was used to read fluorescence with excitation wavelength of 570 nm and emission wavelength of 600 nm settings. One Way ANOVA was performed using IBM SPSS Statistics 22 Software (New York, USA) for statistical analysis ($p < 0.05$).

In Vivo Studies

Cell Culture—Human neuroblastoma KELLY cells (Sigma-Aldrich, St Louis, MO) were maintained in RPMI 1640 (HyClone, Logan, UT) supplemented with 5% fetal bovine serum, 1% a,l-glutamine, 1%OPI, and two mM glutamine in RPMI as previously described[7]. All cells were incubated in a 5% CO_2 atmosphere at 37°C and trypsin-passaged at 80% confluence.

Mouse Orthotopic Neuroblastoma Model—All mouse procedures were performed in accordance with Stanford University's recommendations for the care and use of animals and

were maintained and handled under protocols approved by the Institutional Animal Care and Use Committee (APLAC Protocol # 32942). Seven-week old female NCr nude mice were used to establish an orthotopic neuroblastoma xenograft as previously described[9]. Briefly, mice were anesthetized with intraperitoneal injection of Ketamine 100 mg/kg and Xylazine 10 mg/kg and a transverse incision was made on the left flank. Two μL of phosphate buffered saline (PBS) containing one million KELLY cells were injected into the left adrenal gland. The fascia and skin were closed in separate layers. Non-invasive ultrasound measurements (VisualSonics Vevo 2100, Toronto, Ontario, Canada) were performed on mice anesthetized with isoflurane inhalation following the tumor formation. Animals were euthanized when the tumor volume exceeded 1000 mm^3 and a full necropsy was performed at the time of tumor harvest.

Implantation of Silk Reservoirs—This procedure was previously described[9]. Briefly, animals underwent treatment once the tumor volume reached >100 mm^3 as determined via high frequency ultrasound imaging. The tumor was identified and dissected free from surrounding structures through a left lateral transverse incision. The tumor capsule was incised using cautery and the silk reservoirs with (n=4 for 0.2 mg and n=5 for 0.5 mg cisplatin reservoirs) or without cisplatin (n=3) were inserted into the tumor. The fascia and the skin were then closed in layers. For comparison, the established treatment for preclinical models, adapted from the Children's Oncology Group protocol includes cisplatin administered systemically during courses one, three and five (two mg/kg daily on days one through five)[34].

High Frequency Ultrasound—A VisualSonics Vevo 2100 sonographic probe (Toronto, Ontario, Canada) was used to monitor and measure tumor growth as previously described[31]. Briefly, the mouse was anesthetized with inhalational isoflurane and secured in a prone position for measurements. The ultrasound probe was placed over the left flank to locate the left adrenal gland and the tumor. Serial cross-sectional images (0.076 mm between images) were taken, and 3-D reconstruction tool (Vevo Software v1.6.0, Toronto, Ontario, Canada) was used to calculate the tumor volume. After the implantation of the silk reservoir, tumors were measured every three to four days. To ensure consistency, ultrasound of the animals and tumor volume calculations were performed by the same person (J.Z.) throughout this study.

Statistical Analysis for In Vivo Studies—Tumor sizes and post-operative days were entered into a scatter plot, and a curve of best fit with the associated equation was created for each animal. By entering the desired tumor size (500 mm^3, 600 mm^3, 700 mm^3, or 800 mm^3) into the equation, we solved for the post-operative day using the "goal seek" function under the "what-if analysis" (Microsoft Excel, 2011, version 14.7.4, Redmond, Washington). The post-operative days obtained were compared between different groups using Student's t test, and a p value <0.05 was considered statistically significant.

RESULTS AND DISCUSSION

Intra-tumoral delivery of chemotherapeutics has been recognized as an alternative method for reaching therapeutic drug doses at tumor sites while reducing or eliminating systemic

toxicity. The Gliadel wafer® drew attention to the peri-surgical delivery of chemotherapeutics when it became the first FDA approved intra-tumor implant for glioblastoma treatment. The absence of a local neuroblastoma treatment led us to study the potential for silk-based drug carrier platforms, which can be placed in tumors or in the tumor resection area during surgery and provide sustained chemotherapy to reduce tumor growth or prevent tumor remission. In our previous studies, we have successfully formulated doxorubicin, vincristine and etoposide using different silk platforms such as gels, films, foams, and wafers[7–9, 31]. However, physicochemical properties of cisplatin create difficulties in formulations with conventional dosage forms without the addition of toxic excipients due to the lack of solubility of the drug. We therefore designed reservoir formulations to overcome the solubility issue and encapsulate powdered cisplatin in a silk system to achieve therapeutic doses in the tumor site.

One of the first applications of intra-tumoral cisplatin was using special microcatheters to deliver the drug to glioma tumors, with no morbidity reported for the six months of follow up. However, the authors stated one of the disadvantages of the method was the short exposure time to the drug due to diffusion to the cerebrospinal fluid[35]. To overcome this disadvantage, different approaches have been tested for cisplatin delivery to soft tissue tumors. An injectable, poly (sebacic acid-co-ricinoleic acid ester anhydride) formulation was tested on mouse bladder tumors where cisplatin was detected in the tumor 14 days after treatment[36]. Biodegradable 6-carboxylcellulose implants were used to deliver cisplatin to a group of patients for glioblastoma treatment and higher survival rate was reported. However, 14 out of 17 patients died by the time of publication[37]. Local cisplatin delivery for neuroblastoma treatment is still unexplored with the need of high drug loading, controlled release and adjustable size. We aimed to fulfill these needs with the cisplatin loaded silk reservoir system developed in this study. In these reservoir formulations, silk was used as a shell to carry the drug into the tumor and release the drug as it was cleared from the area. Entrapping cisplatin in powder form helped overcome the limited drug loading and provided 100% control over drug dosing.

FTIR Spectroscopy

Silk proteins change conformation from random coil and alfa helix to β-sheet when treated by water vapor annealing, aqueous alcohol or with salt solutions[38, 39]. The β- sheets act as physical crosslinks and provide mechanical stability and water insolubility to the silk materials[40]. High β-sheet ratio is preferred for controlled release systems with reduced degradation rates. The FTIR spectral regions between 1700–1600 cm^{-1} and 1600–1500 cm^{-1} are assigned to amide I and amide II absorption, respectively. These regions have been widely used for secondary structure analysis of silk as the peaks at 1610–1630 cm^{-1} (amide I) and 1510–1520 cm^{-1} (amide II) are characteristic of silk II secondary structure[32].

We used water vapor annealing to induce β-sheet formation to stabilize the integrity of the reservoirs and FTIR analysis to quantify β-sheet in comparison with alfa helixes, random coils, turns and side chains to confirm the integrity and insolubility of the silk reservoirs (Figure 2). β-sheet content for the silk reservoirs was between 32.6 to 35.8% according to the deconvolution data. No significant differences were observed between the formulations

(p>0.05), indicating that drug loading did not affect the physical structure of the reservoirs. The reservoirs kept their intact form during the 30 day release studies in correlation with the high crystalline structure suggested by the FTIR data.

In Vitro Release Studies

The release from cisplatin reservoirs was dose dependent and the highest dose reservoirs (2 mg) released the drug for the longest period of time (30 days), whereas the low dose reservoir (0.2 mg) release lasted for 4 days (Figure 3). The 2 mg cisplatin reservoirs released 76.9±21.2μg of the drug in the first 2 hours and the drug release showed a linear increase until the 10th day of release, while the total release lasted for 30 days and 65.9% of the total drug was released (Figure 3a). Reservoirs loaded with 1, 0.5 and 0.2 mg drug initially released 26.9±18.0μg, 11.1±10.0μg and 27.9±9.3μg cisplatin and at the end of the release study 77.0%, 67.2% and 26.7% of the drug has been released, respectfully. Released cisplatin at each time point is presented in Figure 3b. Drug release profiles of high and low dose formulations were significantly different from each other at every time point except 2 h (p < 0.05).

Drug release is affected by multiple factors including formulation material (drug binding, degradation rate, swelling), release medium (pH, temperature, enzymes, flow rate), and drug compounds (solubility, charge)[41]. Zeki et al. demonstrated that local treatment with chemotherapy-loaded silk fibroin follows a pattern of diffusion, and that treatment efficacy can be improved by decreasing diffusion distances[8]. Coburn et al. demonstrated the versatility and customizability of silk-loaded reservoirs to deliver tailored amounts of chemotherapy locally[42]. The data showed that in vitro cisplatin release from reservoirs was controlled by drug solubility and diffusion rate, thus the higher drug loading resulted in higher amounts of drug release for longer periods of time as the reservoirs served as a depot for the drug. As drug release is solubility dependent and diffusion controlled, first order release kinetics would be expected to follow zero order release kinetics after the depletion of excess drug in the reservoirs[43]. This release pattern suggests that in vivo release of drug from the reservoirs would be dependent on blood flow and extracellular fluids in the tumor environment. Tumor interstitial fluid pressure is known to be partly responsible for the poor penetration of drugs[44], however. This feature may help by releasing more of the drug from reservoir formulations in vivo. As the release is dependent on cisplatin solubility, reservoirs are expected to release the drug as it gets cleared from the tumor area and sustain tissue drug concentration.

In Vitro Cytotoxicity Studies

Cytotoxicity of cisplatin on KELLY cells was tested using AlamarBlue® assay and LC50 value (lethal dose of cisplatin to kill 50% of the cell population) was calculated based on the linear portion of the cell viability curve (Figure 4a). The data indicated that 3.2 μg/mL cisplatin was required to kill 50% of the cell population, or 50,000 KELLY cells. To determine the formulation efficiency, the cytotoxic effect of the cisplatin loaded silk reservoirs was investigated by exposing the cells to the in vitro release samples. Cell viability over time was calculated following the exposures (Figure 4b). The data showed that 88.4%, 98.3%, 100% and 97.9 % of the cells were killed with the first 2 hours of exposure to

samples of 0.2 mg, 0.5 mg, 1 mg and 2 mg cisplatin loaded reservoirs, respectively. From lowest dose to highest dose, formulations were significantly effective for 2, 10, 16 and 21 days when compared to untreated cells. Two mg cisplatin loaded reservoirs were still able to kill 24.1% of the cells after 21 days. Cytotoxicity data correlated with the results of the in vitro release study, as the higher dose reservoirs were able to release the drug over a longer period of time.

In Vivo Studies

Following neuroblastoma induction in mice, tumors were observed until they reached 100 mm^3. Once the tumor reached 100 mm^3, 0.2 mg cisplatin reservoirs (n=4), 0.5 mg cisplatin reservoirs (n=5), and the control reservoirs (n=3) were implanted into the tumors to determine efficacy. One and two mg cisplatin formulations were also implanted in the animals (n=5), however shortly after implantation the animals died due to toxicity of the high cisplatin dose. This survival data combined with the in vitro release and cytotoxicity data suggest that increasing doses of cisplatin beyond 0.5 mg does not significantly improve cytotoxicity and only serves to increase toxicity. By using lower doses locally, this work and previous work demonstrate decreased toxicity while improving tumor growth suppression as discussed herein[9].

Following implantation of reservoirs, tumor growth was suppressed in the cisplatin reservoir groups relative to control. Tumors treated with 0.5 mg cisplatin loaded silk reservoirs took 17.6 ± 6.4 days to reach 500 mm^3, whereas tumors treated with 0.2 mg cisplatin reservoirs took 4.2 ± 1.8 days and control reservoirs 1.2 ± 0.3 days (p=0.008 and p=0.03, respectively relative to control) (Figure 5). The difference in growth velocity between the cisplatin doses was also significant at this time point (p=0.003). Similarly, significant differences were seen in tumor growth among all reservoir groups in the times tumors took to reach 600 mm^3, 700 mm^3 and 800 mm^3. It took 2.0 ± 0.4 days, 2.8 ± 0.5 days and 3.5 ± 0.6 days for control reservoir tumors to reach 600 mm^3, 700 mm^3 and 800 mm^3, respectively; tumors treated with 0.2 mg cisplatin took 7.2 ± 3.4 days, 8.5 ± 3.7 days and 9.5 ± 3.9 days to reach the same volumes; tumors treated with 0.5 mg cisplatin took 19.4 ± 6.3 days, 21.0 ± 6.2 days and 22.4 ± 6.1 days (Figure 5). No tumor metastasis beyond the primary tumor was observed at the time of tumor harvest.

Sections of formalin-preserved and paraffin-embedded post-intervention tumor sections demonstrated a differential response based on the presence of cisplatin in the reservoir. Hematoxylin and eosin (H&E) staining demonstrated small round blue cells typical of viable neuroblastoma adjacent to the control silk fibroin reservoir (Figure 6). The cisplatin-loaded reservoirs, however, depicted widespread cell death in the tumor adjacent to the reservoir. The silk reservoir causes minimal foreign body reaction within the tumor as a relatively inert material.

During the in vivo studies, following implantation of the reservoirs, the mice were monitored based on their behavior and weight changes as a measure of tolerance to treatment and systemic toxicity. No behavioral or significant weight changes were observed (p>0.05) between the cisplatin reservoir treatments groups compared to the control group. As discussed above, cisplatin has a number of short and long term toxic side effects that

limit its clinical utility[12]. While mice treated with one or two mg doses of cisplatin did not survive for analysis, the mice treated at the lower doses had tumor growth suppression without evidence of systemic toxicity or weight loss. Local therapies with chemotherapy-loaded reservoirs such as this have previously been shown to be less toxic than systemically delivered chemotherapy[9]. The decrease in toxic side effects may allow for higher doses to be delivered locally or more complete treatment adherence.

Advanced stage neuroblastoma is often treated with aggressive, multi-agent neoadjuvant therapy[45], which provides an opportunity for concurrent local therapy with a drug delivery vehicle such as this. This reservoir system could be potentially used to decrease or complement the systemic chemotherapy or other anti-tumor therapies prior to surgery. Additionally, this strategy could be applied to neuroblastoma or other solid tumors at the time of resection. Previous work has demonstrated improved local control and tumor growth suppression when using local, sustained release chemotherapy platforms after an incomplete tumor resection compared to resection alone or combined with IV chemotherapy[31]. More work is needed to translate this model into clinical trials and to determine the clinical benefits. Orthotopic xenografts such as this, however, are ideal for replicating the tumor microenvironment and simulating host response to therapy[46]. The orthotopic xenograft as a preclinical model allows for accurate study of tumor response to diffusion based treatment such as this cisplatin reservoir[47].

CONCLUSIONS

We have designed a sustained release silk reservoir system for cisplatin delivery that can be easily implanted into neuroblastoma tumor resections during surgery. Implantation of the cisplatin loaded silk reservoirs within orthotopic neuroblastoma tumors resulted in a significant decrease in tumor growth. Evaluation of in vivo tissue distribution of the drug and testing on tumors with different focal origins will be needed to further validate the potential clinical value of these formulations.

Supplementary Material

Refer to Web version on PubMed Central for supplementary material.

ACKNOWLEDGEMENTS

REFERENCES

1. Maris JM, Hogarty MD, Bagatell R, Cohn SL. Neuroblastoma. Lancet. 2007;369(9579): 2106–2120. [PubMed: 17586306]

2. Murphy JM, La Quaglia MP. Advances in the surgical treatment of neuroblastoma: a review. Eur J Pediatr Surg. 2014;24(6): 450–456. [PubMed: 25486413]

3. Schwartz CL. Long-term survivors of childhood cancer: the late effects of therapy. Oncologist. 1999;4(1): 45–54. [PubMed: 10337370]

4. Coku J, Scadden EO, Liu KN, et al. Chemotherapy resistance in pediatric neuroblastoma is associated with reduced ER -mitochondria tethering. Cancer Research. 2016;76.

5. Tanos R, Karmali D, Nalluri S, Goldsmith KC. Select Bcl-2 antagonism restores chemotherapy sensitivity in high-risk neuroblastoma. BMC cancer. 2016;16: 97. [PubMed: 26874859]

6. Wolinsky JB, Colson YL, Grinstaff MW. Local drug delivery strategies for cancer treatment: Gels, nanoparticles, polymeric films, rods, and wafers. Journal of Controlled Release. 2012;159(1): 14–26. [PubMed: 22154931]

7. Yavuz B, Zeki J, Coburn JM, et al. In vitro and in vivo evaluation of etoposide - silk wafers for neuroblastoma treatment. J Control Release. 2018;285: 162–171. [PubMed: 30018030]

8. Zeki J, Taylor JS, Yavuz B, et al. Disseminated injection of vincristine-loaded silk gel improves the suppression of neuroblastoma tumor growth. Surgery. 2018.

9. Coburn J, Harris J, Zakharov AD, et al. Implantable chemotherapy-loaded silk protein materials for neuroblastoma treatment. International Journal of Cancer. 2017;140(3): 726–735. [PubMed: 27770551]

10. Harris J, Klonoski SC, Chiu B. Clinical Considerations of Focal Drug Delivery in Cancer Treatment. Current drug delivery. 2017;14(5): 588–596. [PubMed: 28240175]

11. Zhu W, Li Y, Liu L, Chen Y, Wang C, Xi F. Supramolecular hydrogels from cisplatin-loaded block copolymer nanoparticles and alpha-cyclodextrins with a stepwise delivery property. Biomacromolecules. 2010;11(11): 3086–3092. [PubMed: 20958000]

12. Wang D, Lippard SJ. Cellular processing of platinum anticancer drugs. Nat Rev Drug Discov. 2005;4(4): 307–320. [PubMed: 15789122]

13. Alam N, Khare V, Dubey R, et al. Biodegradable polymeric system for cisplatin delivery: development, in vitro characterization and investigation of toxicity profile. Materials science & engineering C, Materials for biological applications. 2014;38: 85–93. [PubMed: 24656356]

14. Hagiwara A, Takahashi T, Sawai K, et al. Clinical trials with intraperitoneal cisplatin microspheres for malignant ascites--a pilot study. Anti-cancer drug design. 1993;8(6): 463–470. [PubMed: 8286013]

15. Moreno D, Zalba S, Navarro I, Tros de Ilarduya C, Garrido MJ. Pharmacodynamics of cisplatin-loaded PLGA nanoparticles administered to tumor-bearing mice. Eur J Pharm Biopharm. 2010;74(2): 265–274. [PubMed: 19883755]

16. Newman MS, Colbern GT, Working PK, Engbers C, Amantea MA. Comparative pharmacokinetics, tissue distribution, and therapeutic effectiveness of cisplatin encapsulated in long-circulating, pegylated liposomes (SPI-077) in tumor-bearing mice. Cancer chemotherapy and pharmacology. 1999;43(1): 1–7. [PubMed: 9923534]

17. Duan X, He C, Kron SJ, Lin W. Nanoparticle formulations of cisplatin for cancer therapy. Wiley interdisciplinary reviews Nanomedicine and nanobiotechnology. 2016;8(5): 776–791. [PubMed: 26848041]

18. Uehara T, Watanabe H, Itoh F, et al. Nephrotoxicity of a novel antineoplastic platinum complex, nedaplatin: a comparative study with cisplatin in rats. Arch Toxicol. 2005;79(8): 451–460. [PubMed: 15856183]

19. Deurloo MJ, Kop W, van Tellingen O, Bartelink H, Begg AC. Intratumoural administration of cisplatin in slow-release devices: II. Pharmacokinetics and intratumoural distribution. Cancer chemotherapy and pharmacology. 1991;27(5): 347–353. [PubMed: 1998994]

20. Oun R, Plumb JA, Wheate NJ. A cisplatin slow-release hydrogel drug delivery system based on a formulation of the macrocycle cucurbit[7]uril, gelatin and polyvinyl alcohol. Journal of inorganic biochemistry. 2014;134: 100–105. [PubMed: 24595010]

21. Rockwood DN, Preda RC, Yucel T, Wang XQ, Lovett ML, Kaplan DL. Materials fabrication from Bombyx mori silk fibroin. Nat Protoc. 2011;6(10): 1612–1631. [PubMed: 21959241]

22. Jewell M, Daunch W, Bengtson B, Mortarino E. The development of SERI (R) Surgical Scaffold, an engineered biological scaffold. Pharmaceutical Science to Improve the Human Condition: Prix Galien 2014. 2015;1358: 44–55.

23. Holland C, Numata K, Rnjak-Kovacina J, Seib FP. The Biomedical Use of Silk: Past, Present, Future. Adv Healthc Mater. 2019;8(1).

24. Yucel T, Lovett ML, Keplan DL. Silk-based biomaterials for sustained drug delivery. Journal of Controlled Release. 2014;190: 381–397. [PubMed: 24910193]

25. Kim SY, Naskar D, Kundu SC, et al. Formulation of Biologically-Inspired Silk-Based Drug Carriers for Pulmonary Delivery Targeted for Lung Cancer. Sci Rep-Uk. 2015;5.

26. Seib FP, Pritchard EM, Kaplan DL. Self-Assembling Doxorubicin Silk Hydrogels for the Focal Treatment of Primary Breast Cancer. Adv Funct Mater. 2013;23(1): 58–65. [PubMed: 23646041]

27. Seib FP, Kaplan DL. Doxorubicin-loaded silk films: Drug-silk interactions and in vivo performance in human orthotopic breast cancer. Biomaterials. 2012;33(33): 8442–8450. [PubMed: 22922025]

28. Coburn JM, Na E, Kaplan DL. Modulation of vincristine and doxorubicin binding and release from silk films. Journal of Controlled Release. 2015;220: 229–238. [PubMed: 26500149]

29. Seib FP, Coburn J, Konrad I, et al. Focal therapy of neuroblastoma using silk films to deliver kinase and chemotherapeutic agents in vivo. Acta Biomaterialia. 2015;20: 32–38. [PubMed: 25861948]

30. Yucel T, Lovett ML, Giangregorio R, Coonahan E, Kaplan DL. Silk fibroin rods for sustained delivery of breast cancer therapeutics. Biomaterials. 2014;35(30): 8613–8620. [PubMed: 25009069]

31. Chiu B, Coburn J, Pilichowska M, et al. Surgery combined with controlled-release doxorubicin silk films as a treatment strategy in an orthotopic neuroblastoma mouse model. Brit J Cancer. 2014;111(4): 708–715. [PubMed: 24921912]

32. Hu X, Kaplan D, Cebe P. Determining beta-sheet crystallinity in fibrous proteins by thermal analysis and infrared spectroscopy. Macromolecules. 2006;39(18): 6161–6170.

33. Anilanmert B, Yalcin G, Arioz F, Dolen E. The spectrophotometric determination of cisplatin in urine, using o-phenylenediamine as derivatizing agent. Anal Lett. 2001;34(1): 113–123.

34. Teitz T, Stanke JJ, Federico S, et al. Preclinical Models for Neuroblastoma: Establishing a Baseline for Treatment. Plos One. 2011;6(4).

35. Bouvier G, Penn RD, Kroin JS, Beique RA, Guerard MJ, Lesage J. Stereotactic administration of intratumoral chronic chemotherapy of recurrent malignant gliomas. Applied neurophysiology. 1987;50(1–6): 223–226. [PubMed: 3329850]

36. Shikanov A, Shikanov S, Vaisman B, Golenser J, Domb AJ. Cisplatin tumor biodistribution and efficacy after intratumoral injection of a biodegradable extended release implant. Chemotherapy research and practice. 2011;2011: 175054.

37. Sheleg SV, Korotkevich EA, Zhavrid EA, et al. Local chemotherapy with cisplatin-depot for glioblastoma multiforme. Journal of neuro-oncology. 2002;60(1): 53–59. [PubMed: 12416546]

38. Chen X, Shao Z, Knight DP, Vollrath F. Conformation transition kinetics of Bombyx mori silk protein. Proteins. 2007;68(1): 223–231. [PubMed: 17436322]

39. Ling S, Qi Z, Knight DP, Shao Z, Chen X. Synchrotron FTIR microspectroscopy of single natural silk fibers. Biomacromolecules. 2011;12(9): 3344–3349. [PubMed: 21790142]

40. Qin Z, Buehler MJ. Cooperative deformation of hydrogen bonds in beta-strands and beta-sheet nanocrystals. Phys Rev E. 2010;82(6).

41. Fu Y, Kao WJ. Drug release kinetics and transport mechanisms of non-degradable and degradable polymeric delivery systems. Expert Opin Drug Deliv. 2010;7(4): 429–444. [PubMed: 20331353]

42. Coburn JM, Harris J, Cunningham R, Zeki J, Kaplan DL, Chiu B. Manipulation of variables in local controlled release vincristine treatment in neuroblastoma. J Pediatr Surg. 2017;52(12): 2061–2065. [PubMed: 28927981]

43. Dash S, Murthy PN, Nath L, Chowdhury P. Kinetic Modeling on Drug Release from Controlled Drug Delivery Systems. Acta poloniae pharmaceutica. 2010;67(3): 217–223. [PubMed: 20524422]

44. Welter M, Rieger H. Interstitial fluid flow and drug delivery in vascularized tumors: a computational model. Plos One. 2013;8(8): e70395. [PubMed: 23940570]

45. Maris JM, Hogarty MD, Bagatell R, Cohn SL. Neuroblastoma. Lancet. 2007;369(9579): 2106–2120. [PubMed: 17586306]

46. Khanna C, Jaboin JJ, Drakos E, Tsokos M, Thiele CJ. Biologically relevant orthotopic neuroblastoma xenograft models: primary adrenal tumor growth and spontaneous distant metastasis. In vivo (Athens, Greece). 2002;16(2): 77–85.

47. Zeki J, Taylor JS, Yavuz B, et al. Disseminated injection of vincristine-loaded silk gel improves the suppression of neuroblastoma tumor growth. Surg. 2018;164(4): 909–915.
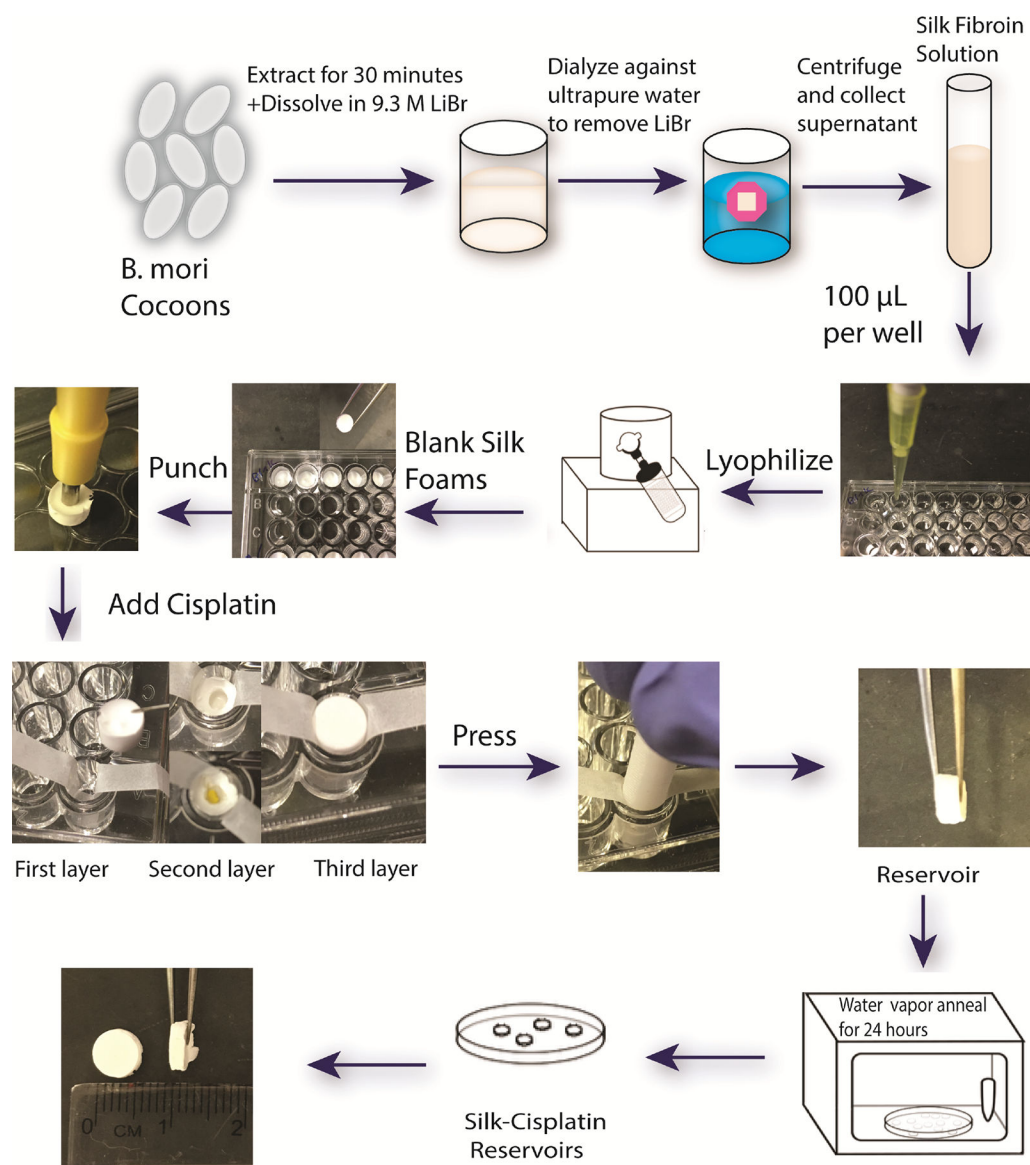
Figure 1.
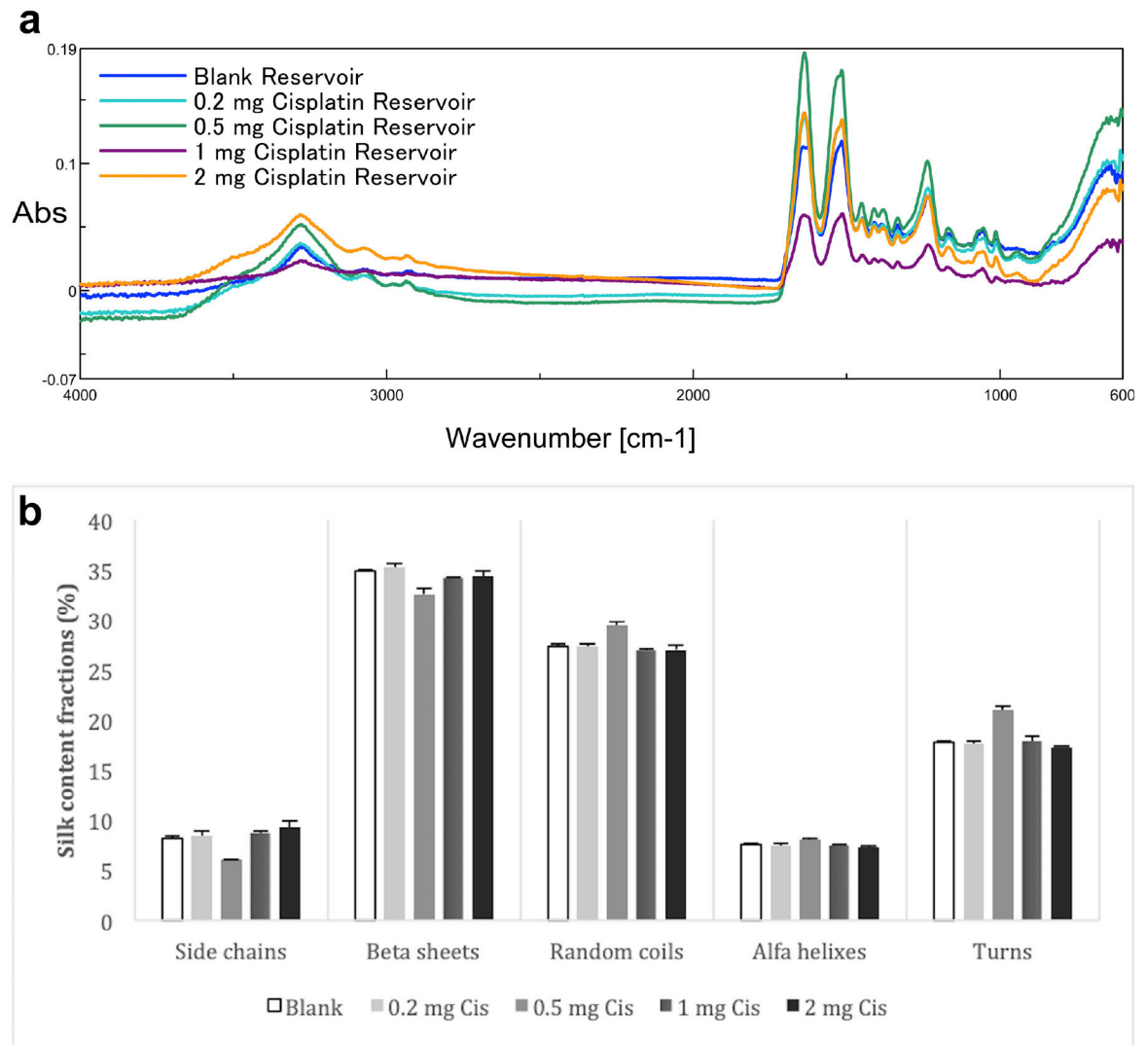Schematic of cisplatin loaded silk reservoir preparation.

a

b

Figure 2.

a) FTIR spectra of silk reservoir formulations

b) Silk content fraction percentages in reservoir formulations based on FTIR spectroscopy. There were no significant differences between formulations in terms of silk content fractions (n=3, p<0.05)).
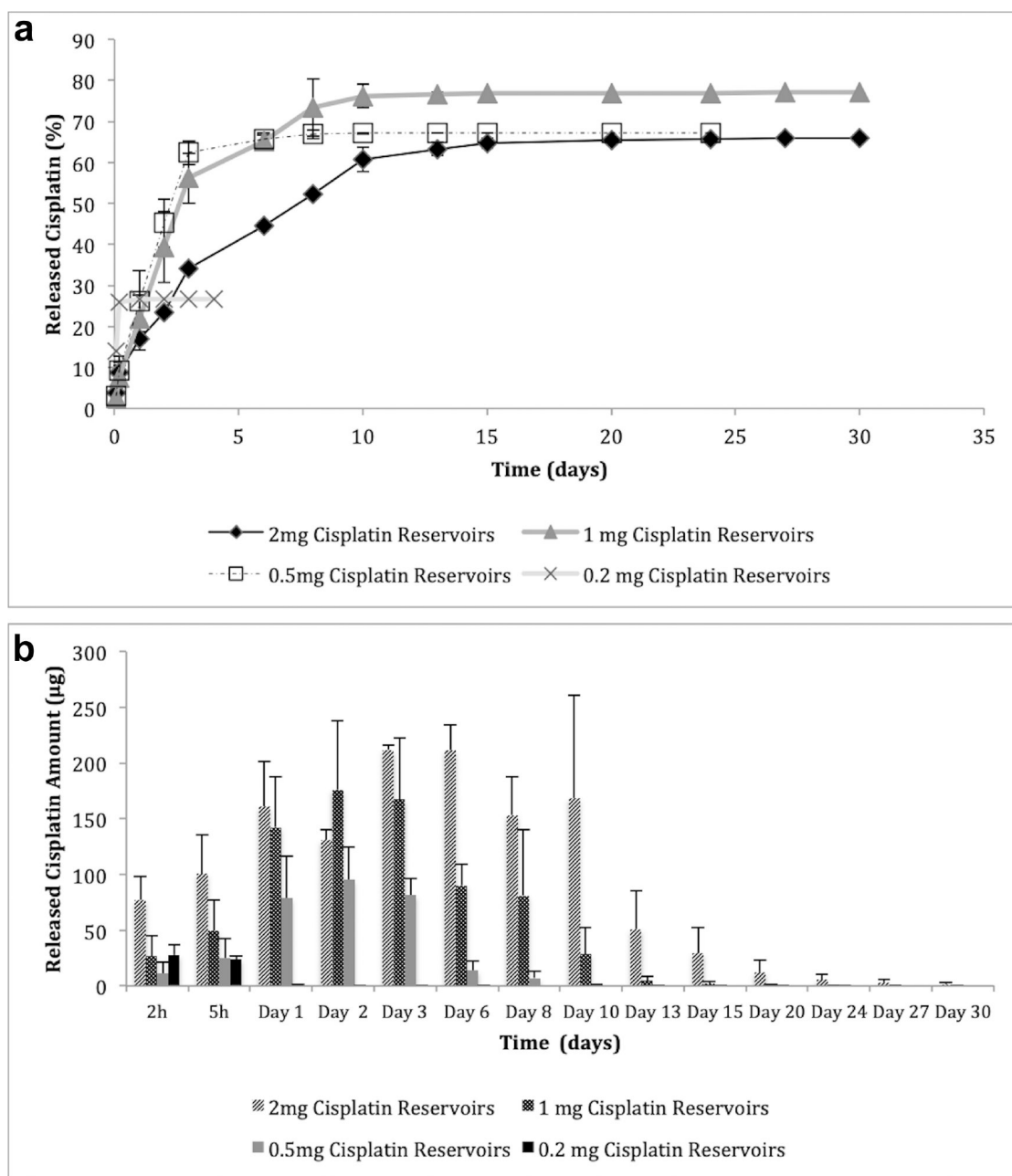
Figure 3.

Cisplatin release from silk reservoirs as a function of time (n=3)

a) Cumulative cisplatin release percentage over the time,

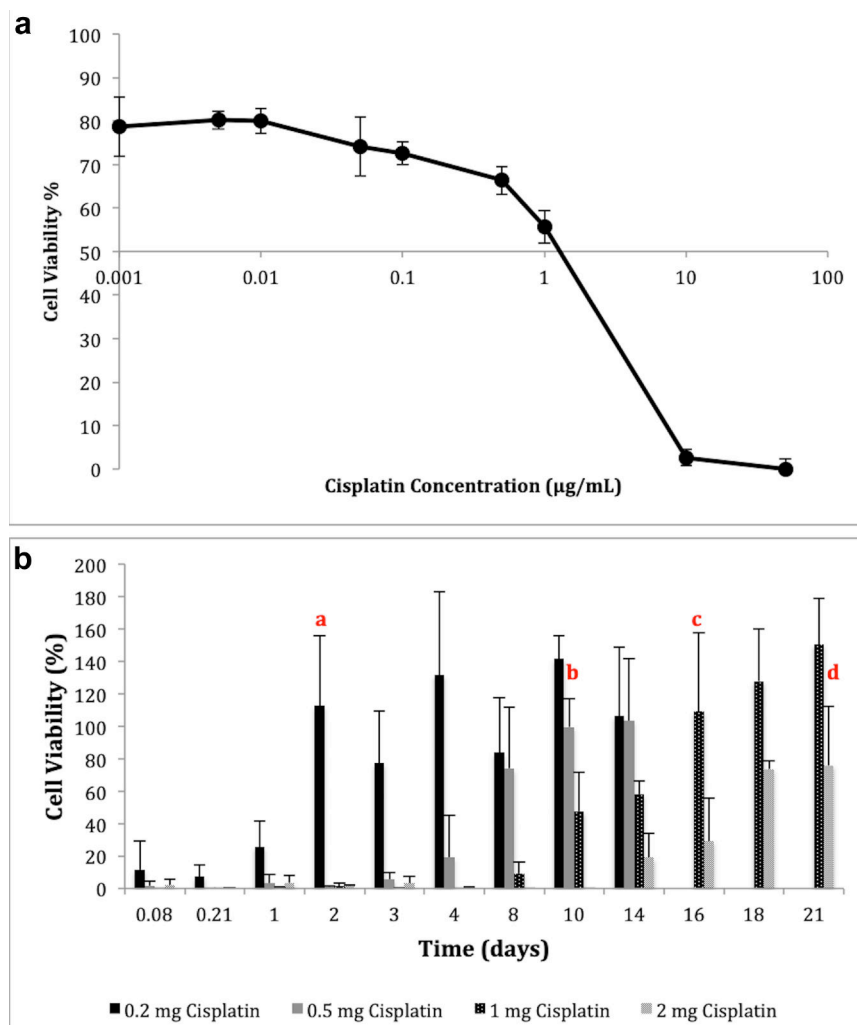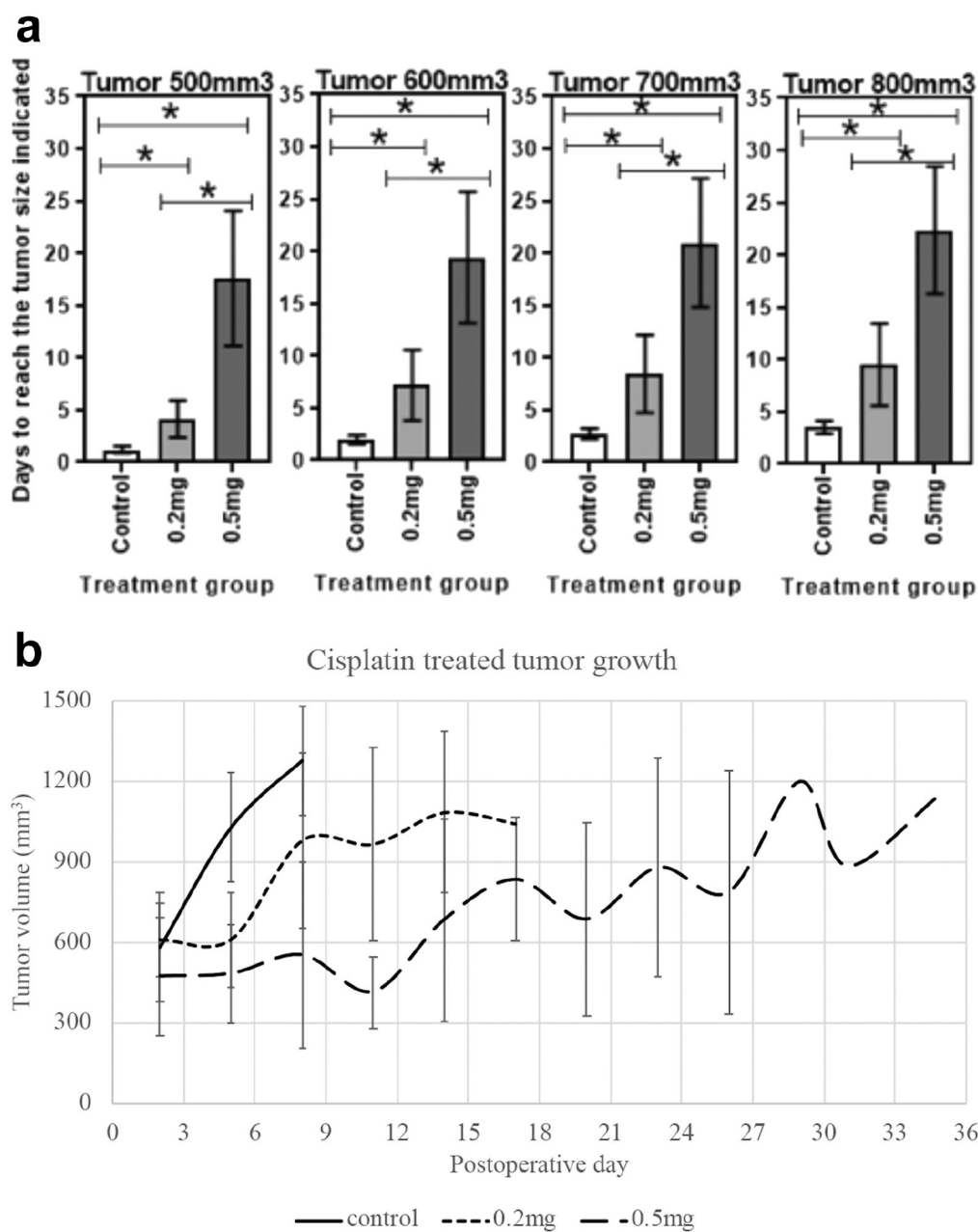b) Released cisplatin amounts at each time point

Figure 4.
Cisplatin cytotoxicity with KELLY cells (n=3) (a) Dose dependent cisplatin cytotoxicity (LC50), (b) long term cytotoxicity of cisplatin loaded silk reservoirs (significantly effective until the time point labeled with a,b,c,d where a) 0.2 mg, b) 0.5 mg, c) 1 mg and d) 2 mg cisplatin, $p<0.05$).

Figure 5.
a) Days to reach tumor volumes 500 mm^3, 600 mm^3, 700 mm^3, and 800 mm^3 after implantation of cisplatin or control reservoirs. b) Tumor size over time based on treatment group.
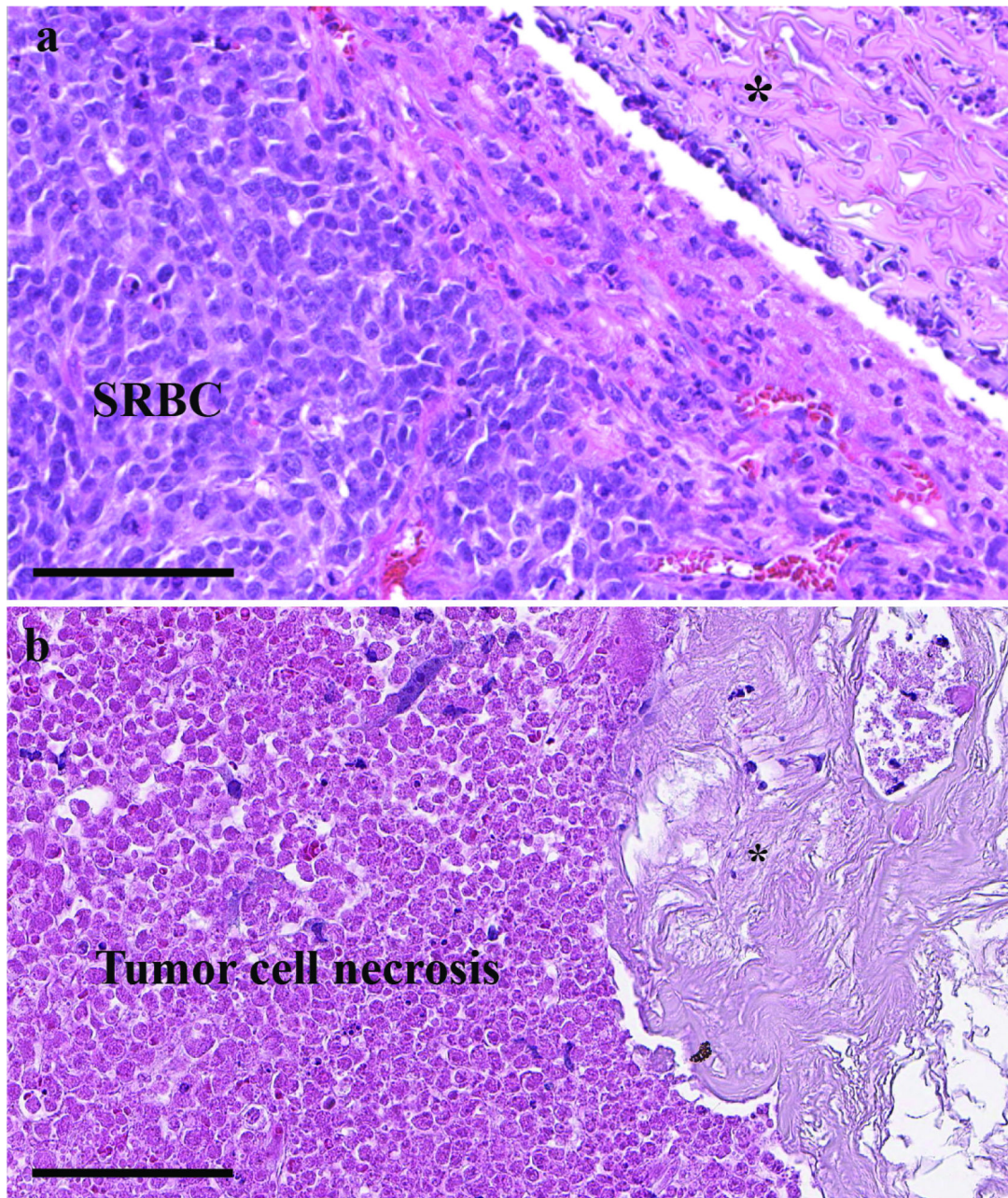
Figure 6.
H&E staining of neuroblastoma xenograft tumor demonstrating (a) viable small round blue cells (SRBC) adjacent to the control silk reservoir (top right corner) and (b) abundant cell necrosis adjacent to silk reservoir loaded with 0.5 mg cisplatin. Asterisk (*) indicates the location of the silk reservoirs. The control and cisplatin-loaded reservoirs show minimal foreign body type reaction, with an absence of infiltrating lymphocytes. Both images are 400 X magnification; scale bar represents 100 μm.